ACS APPLIED MATERIALS & INTERFACES

Research Article

www.acsami.org

Copper Shell Networks in Polymer Composites for Efficient Thermal Conduction

Seunggun Yu,[†,‡] Jang-Woo Lee,[†] Tae Hee Han,*[,§] Cheolmin Park,[‡] Youngdon Kwon,[∥] Soon Man Hong,[†] and Chong Min Koo*[,†,⊥]

[†]Center for Materials Architecturing, Korea Institute of Science and Technology, Seoul 136-791, Republic of Korea

[‡]Department of Materials Science and Engineering, Yonsei University, Seoul 120-749, Republic of Korea

[§]Department of Organic and Nano Engineering, Hanyang University, Seoul 133-791, Republic of Korea

[∥]School of Chemical Engineering, Sungkyunkwan University, Suwon 440-746, Republic of Korea

[⊥]Nanomaterials Science and Engineering, University of Science and Technology, Daejeon 305-350, Republic of Korea

Supporting Information

ABSTRACT: Thermal management of polymeric composites is a crucial issue to determine the performance and reliability of the devices. Here, we report a straightforward route to prepare polymeric composites with Cu thin film networks. Taking advantage of the fluidity of polymer melt and the ductile properties of Cu films, the polymeric composites were created by the Cu metallization of PS bead and the hot press molding of Cu-plated PS beads. The unique three-dimensional Cu shell-networks in the PS matrix demonstrated isotropic and ideal conductive performance at even extremely low Cu contents. In contrast to the conventional simple melt-mixed Cu beads/PS composites at the same concentration of 23.0 vol %, the PS composites with Cu shell networks indeed revealed 60 times larger thermal conductivity and 8 orders of magnitude larger electrical conductivity. Our strategy offers a straightforward and high-throughput route for the isotropic thermal and electrical conductive composites.

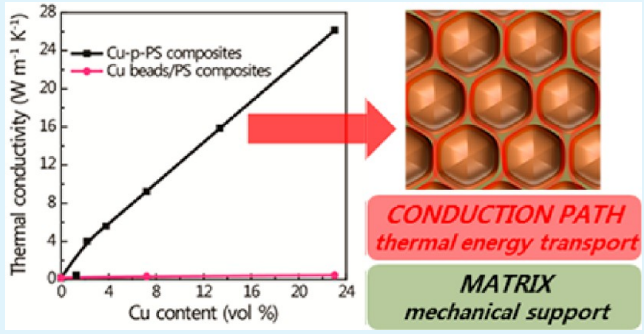

KEYWORDS: *percolation, composites, electroless plating, core−shell, thermal conductivity, electrical conductivity*

INTRODUCTION

Thermal conduction properties of polymeric composites were investigated in an effort to control the heat dissipation of polymer matrix component. The results are directly related to the performance, lifetime, and reliability of a variety of devices including LED, aerospace systems, microelectronics, and photovoltaics.[1,2] Previous research efforts have indicated that thermal conductivity of polymeric composites, made of polymeric matrix and metal,[3,4] inorganic materials,[5−7] or carbonaceous fillers,[8−12] is mainly governed by the type and shape of fillers, because most thermally conductive fillers have the thermal conductivity several order larger than a thermally insulating polymer matrix.[13,14]

Achievement of continuous percolation structure of fillers at low concentrations in a polymer matrix is the most crucial matter for efficient thermal energy transportation of polymer composites.[4,9,15] Below the percolation threshold concentration of fillers in polymeric matrix, the thermal conductivity of composite increases in a limited way with increasing the filler content, because fillers are dispersed in isolated or passivated phase with thermally insulating polymer matrix. Above the critical concentration, however, the thermal conductivity of the composite exponentially increases with an increase in the filler content due to the formation of the continuous percolation architecture of the fillers with large thermal conductivity. The high filler content of above 60−70 vol % could provide a continuous heat conduction path of fillers in the polymer composite.[16−19] Unfortunately, the high filler loading makes processing difficult and increases the cost.

Many studies reported that addition of filler with large aspect ratio in shape and controlling orientation of particles in the polymer composite result in reduction in percolation concentration and enhance the anisotropic thermal conductivity behavior.[19−23] Several research groups reported that long carbon fibers were stacked in the polymer composites to construct one-directional continuous heat conduction pathway.[24−27] However, most composite systems could not be used as a general way not only to reduce the percolation threshold concentration but also to improve isotropic increase in thermal conductivity.

In this work, we report a straightforward route to prepare polymeric composites with highly percolated Cu thermal

Received: July 26, 2013
Accepted: October 25, 2013
Published: October 25, 2013

conduction pathway at extremely low Cu concentration via a simple metallization of polymer beads followed by forming through compression molding process. To date, the continuous metal networks in polymeric matrix have been applied to reduce electrical resistivity.[28,29] Unlike those previous reports, polymer beads with thin metal shell were readily formed with a continuous Cu pathway for the dissipation of thermal energy in the composite via a simple process in this work. Our robust strategy for highly thermal conductive nanocomposites offers not only the technologically advanced process for small content of expensive fillers but also an extremely simple model system for the isotropic thermal conductive composites with high thermal conductivity.

EXPERIMENTAL SECTION

Materials. Polystyrene (PS) beads were purchased from Microbeads AS (Dynoseeds R TS 40). The average size and molecular weight of PS beads were approximately 40.5 μm and 164 kg mol^{-1}, respectively. Copper beads with the diameter of 10 μm were purchased from Sigma Aldrich, U.S.A. Water was deionized using a Milli-Q Plus System (Millipore Corp., U.S.A.). Sulfuric acid with 95% purity was pruchased from Junsei Chemical, South Korea. Pretreatment reagents, including conditioner, sensitizer, activator, and accelerator and electroplating solution were purchased from KPM Tech Co., Ltd., South Korea.

Preparation of Electroless Cu-Plated PS Beads and Cu-Plated PS Composites. The commercially available thermoplastic PS microbeads were uniformly coated with Cu thin film through electroless plating method, as shown in Supporting Information Figure S1. PS beads were treated with ozone for 40 min, and then the plating process was conducted in the electroless plating bath for 120 min/cycle at 35 °C. Thin Cu shell on the PS beads was naturally electroless-plated from Pd catalytic sites in the nucleation and growth manner. The thickness of the Cu shell on the PS beads was controlled through repetition of electroless plating cycles. For the fabrication of Cu-plated PS composites, the Cu-plated PS beads were put into stainless mold with diameter of 12.6 mm and hot-pressed with pressure of 5.6 MPa at 260 °C for 60 min using a compression molding machine (Auto series, Carver, Inc., U.S.A.). Hot-pressed composite samples with a thickness of 2 mm were utilized to measure the values of thermal and electrical conductivities. For comparison, Cu beads/PS composites were prepared through compression molding of a simple mixture of PS beads and Cu beads with a diameter of 10 μm at 260 °C.

Characterization. The morphologies of PS beads, Cu-plated PS beads, and Cu-plated PS composites were analyzed using a field emission scanning electron microscope (FE-SEM, FEI Inspect F50, FEI Inc.). The contents of Cu and PS in the Cu-plated PS beads were calculated using thermogravimetric analysis technique (TGA, Q-50, TA Instruments Inc., U.S.A.). Thermal conductivity of the composites was measured using the laser flash method (LFA-447, Netzsch, Germany) based on xenon flash lamp source at room temperature. The thermal diffusivity and the specific heat capacity were determined from this technique compared with pyroceramic reference sample. Thermal conductivity was determined from the equation $k = T_d \times \rho \times C_p$, where T_d, ρ, and C_p are the thermal diffusivity (mm^2 s^{-1}), density (g cm^{-3}), and specific heat capacity (J kg^{-1} K^{-1}), respectively. For the heating and cooling cycle test, the composite and pristine PS were heated up to 130 °C with 5 °C min^{-1} and naturally cooled to room temperature. Electrical conductivity values of the composites were measured with the sheet resistance using a four-point-probe measurement system (CRESBOX, Napson, Japan).

RESULTS AND DISCUSSION

Figure 1a shows schematic illustration of the fabrication process of Cu-plated polystyrene (Cu-p-PS) composite. The PS microbeads were uniformly coated with Cu thin film using

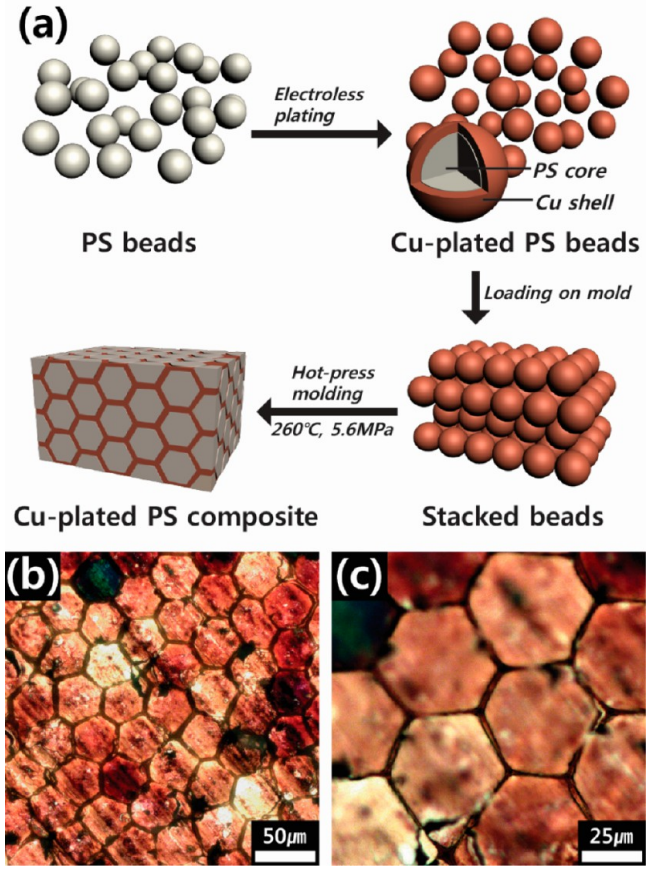

Figure 1. (a) Schematic illustration of fabrication process of Cu-plated PS composite and (b) low and (c) high magnification optical microscope images of Cu-plated PS composite.

electroless plating method in which Cu metal shell on the PS beads was spontaneously deposited from Pd catalytic sites in the nucleation and growth manner (see the detailed procedure of electroless Cu deposition on the PS beads in Supporting Information Figure S1). The thickness of the Cu shell on the PS beads was controlled through the repetition of electroless plating cycle. The Cu-p-PS_3 code represents Cu-p-PS beads prepared through the 3 times repetition of electroless plating. The morphology, thickness, and content of Cu on the PS beads are shown in the SEM micrographs (Supporting Information Figure S2) and TGA thermograms (Supporting Information Figure S3) and are listed in Supporting Information Table S1. The electroless deposition provided uniform Cu thin layers on the PS beads. The volume fraction of Cu shell on PS beads, calculated from the TGA results, increased from 1.3, 2.2, 3.8, 7.2, and 13.4 to 23.0 vol % as the plating cycle was repeated 1, 2, 3, 7, and 10 to 17 times, respectively. Cu-p-PS composites were fabricated through direct compression molding of Cu-p-PS beads at 260 °C, which is quite above melting temperature of PS. Under high pressure of 5.6 MPa at elevated temperature, Cu-p-PS beads were squeezed that formed honeycomb-like shape, as shown in Figure 1b,c. Finally, Cu-p-PS beads were directly compressed to form Cu-p-PS composites by themselves without addition of extra polymer matrix. SEM micrographs of freeze fractured sides in Figure 2 indicate how the PS melt flows out of the Cu-p-PS beads. Under high pressure at elevated temperature, some parts of ductile Cu shell burst and formed hole-like crack for the release of PS melt, as indicated with white arrows in Figure 2c. The thermoplastic PS melt

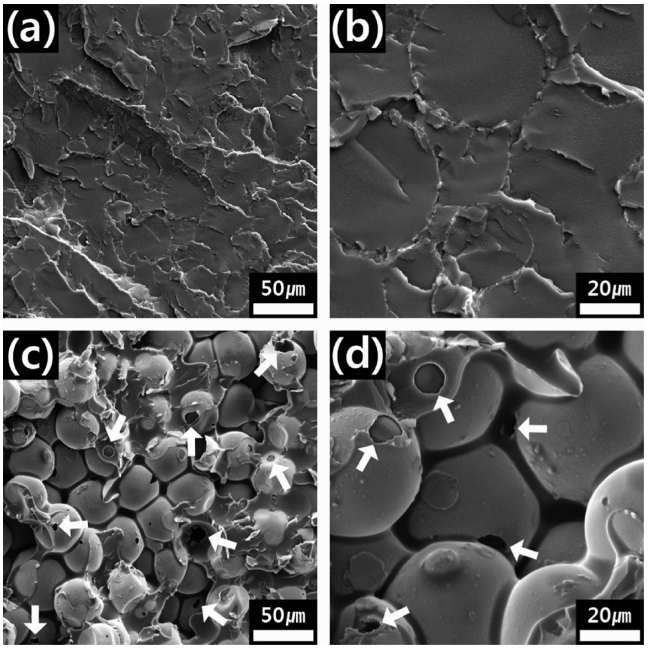

Figure 2. SEM micrographs of freeze fractured sides of Cu-p-PS composites of Cu contents of 1.3 vol % (a, b) and 7.2 vol % (c, d). White arrows in (c) and (d) indicate the hole-like cracks, formed during hot-pressing, in Cu shells for leakage of PS melt.

flowed out from the hole-like crack of Cu shell on the Cu-plated PS beads and faced to neighboring PS or Cu shell. The leakage of the PS melt caused the filling of the vacant space between beads and the leaked PS melt played as a matrix in the Cu-p-PS composites. In addition, the polymeric multidomain structures in Figure 2c are due to Cu shells embedded in the composites.

Figure 3a–d shows a cross-sectional view of SEM micrographs of the Cu-p-PS composites. Molten PS perfectly filled

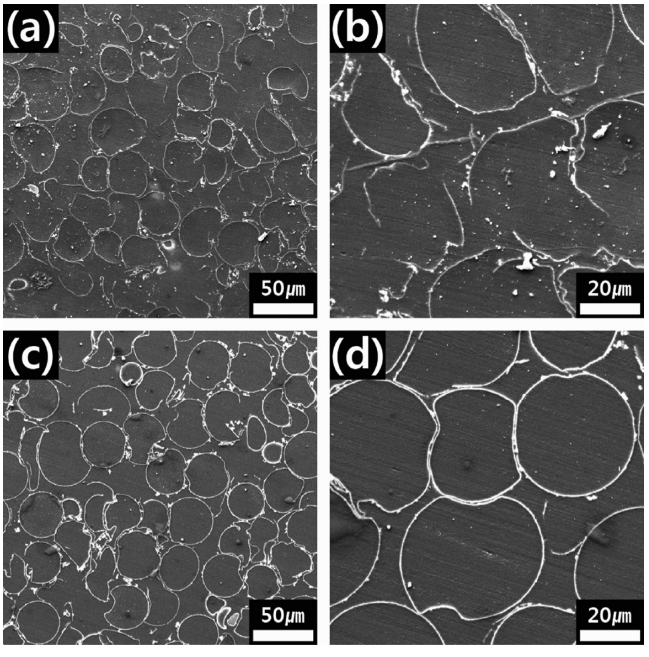

Figure 3. SEM micrographs of cross-sectional view of Cu-p-PS composites of Cu contents of 1.3 vol % (a, b) and 2.2 vol % (c, d).

the empty spaces between Cu-p-PS beads without leaving any voids and thin Cu shells were deformed and interconnected without severe collapse or interruption in the composites. However, at a low Cu content of 1.3 vol % (Figure 3a,b), Cu shells were largely deformed and partially damaged to be interdisconnected in the composites. At the Cu content larger than 2.2 vol % (Figure 3c,d and Supporting Information Figure S5), thick Cu shells were continuously interconnected without any damage in the composite. Formation of the three-dimensional well-interconnected percolation structure of Cu shells without complete failure in the composite was attributed to the unique ductility of Cu metal.

Figure 4a shows the thermal conductivity value variations of Cu-p-PS and Cu beads/PS composites. Neat PS revealed

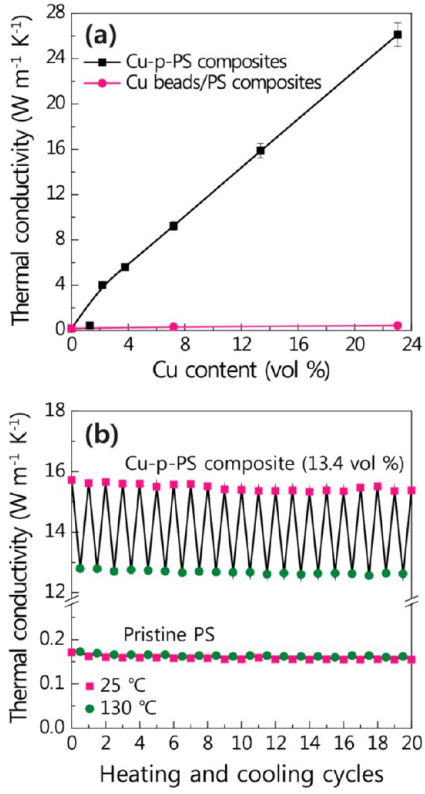

Figure 4. (a) Thermal conductivity of Cu-p-PS and Cu beads/PS composites at various Cu contents and (b) thermal conductivity of Cu-p-PS composites of Cu contents of 13.4 vol % at temperature dependent cycle test repeated with heating and cooling cycles. Each point is connected with a straight line.

thermal conductivity of 0.18 W m^{-1} K^{-1}. Thermal conductivity of Cu-p-PS composites almost linearly increased with an increase in Cu content. The Cu-p-PS composites with Cu content of 23.0 vol % exhibited nearly 145 times larger thermal conductivity (26.14 W m^{-1} K^{-1}) than neat PS. For the comparison, Cu beads/PS composites were prepared through a simple melt-mixing of PS beads and Cu beads with the diameter of 10 μm (see the representative cross-sectional SEM micrograph of Cu beads/PS composite in Supporting Information Figure S6). Unlike Cu-p-PS composites, Cu bead/PS composites hardly showed increase in thermal conductivity. Copper beads/PS composites with 23.0 vol % Cu had thermal conductivity of 0.45 W m^{-1} K^{-1}. It was ascribed to the morphology difference of Cu fillers in the composites. Cu-p-PS composites formed a three-dimensional

Cu shell network even at low Cu content, while Cu beads/PS composites just included the isolated Cu beads in the PS matrix even at quite high Cu content. Interestingly, the thermal conductivity of Cu-p-PS composite linearly increased with an increase in Cu content from very low content of 2.2 vol %, which is often found in the composites systems having continuous heat conduction pathways for the thermal conduction.[9,30,31] The Cu-p-PS composite with the Cu content of 1.3 vol % had the thermal conductivity of 0.46 W m^{-1} K^{-1}, which was slightly deviated from the linear relationship between Cu content and thermal conductivity. This was ascribed to the limit of the electroless plating method in which, at low Cu loading, the imperfectness of the plated Cu layer appeared, due to Cu deposition through the nucleation and growth mechanism, as shown in Figure 3a. Also, the electrical conductivity values variations of Cu-p-PS and Cu beads/PS composites were compared to demonstrate the continuity of Cu shell in the composite as shown in Supporting Information Figure S7. Like the result of thermal conductivities, at the same Cu content of 23.0 vol %, the Cu-p-PS composite revealed electrical conductivity of 4.9×10^3 S cm^{-1}, 8 orders of magnitude larger than that of the Cu beads/PS composite (7.2×10^{-5} S cm^{-1}).

Figure 4b shows the structural stability of the prepared composites at various temperature conditions. During the heating and cooling cycle between 130 and 25 °C, the composites with Cu contents of 13.4 vol % maintained their initial thermal conductivity, even after 20 cycles. We note that the thermal conductivity of the composite at room temperature is higher than at 130 °C due to the temperature dependency of thermal conduction. As shown in Supporting Information Figure S8, the thermal conductivity of Cu-p-PS composites was decreased with increasing temperature to 130 °C as easily found in neat Cu metal.[13] These results reflect that the Cu film networks are the major pathway for the thermal conduction. The structural stability of composites was confirmed in Supporting Information Figure S9. In the cross-sectional view, the internal structure of the Cu-p-PS composite is well-maintained without severe breaking or cracking of the Cu shell network even after the thermal cycle test.

As a result, the Cu-p-PS composites fabricated via a simple metallization of polymer beads followed by compression molding provided a unique and versatile way to prepare polymeric composites with highly percolated Cu thermal conduction pathway at extremely low Cu concentration. Due to the unique structural feature, Cu shells on the PS beads inevitably contact with Cu shell on the adjacent beads to construct the percolated Cu framework regardless of the Cu content, which offers an efficient thermal and electrical conductive pathway.

CONCLUSIONS

We demonstrated a straightforward and versatile route to prepare polymer composites with highly percolated Cu thermal conduction pathway at extremely low Cu content via a simple metallization of polymer beads followed by compression molding. Composites of Cu-p-PS readily formed continuous Cu pathway at very low Cu content for the effective transport of thermal and electrical energy. Because of this unique structural feature, the Cu-p-PS composites indeed revealed 60 times larger thermal conductivity and 8 orders of magnitude larger electrical conductivity than simple melt-mixed Cu beads/PS composite at the same Cu content of 23.0 vol %. Our robust strategy for highly thermal conductive nanocomposites offers not only the technologically advanced process for low loading ratio of expensive fillers but also an extremely simple model system for the isotropic conductive composites with high thermal and electrical conductivities.

ASSOCIATED CONTENT

Supporting Information

Preparation of electroless Cu-plated PS particles was introduced in a detailed manner, and the supplementary figures are provided. This information is available free of charge via the Internet at http://pubs.acs.org.

AUTHOR INFORMATION

Corresponding Authors

*Tel.: +82-2-958-6872. Fax: +82-2-958-5309. E-mail: koo@kist.re.kr (C.M.K.).

*E-mail: than@hanyang.ac.kr (T.H.H.).

Notes

The authors declare no competing financial interest.

ACKNOWLEDGMENTS

This work was supported by a grant from the Fundamental R&D Program for Technology of World Premier Materials funded by the Ministry of Knowledge Economy (MKE) and was partially supported by the Institute for Multidisciplinary Convergence of Materials (IMCM) of the Korea Institute of Science and Technology (KIST) and the research fund of Hanyang University (HY-2013).

ABBREVIATIONS

PS, polystyrene; FE-SEM, field emission scanning electron microscopy; TGA, thermogravimetric analysis; Cu-p-PS, Cu-plated polystyrene

REFERENCES

(1) Tong, X. C. *Development and Application of Advanced Thermal Management Materials*; Springer: New York, 2011; p 527.
(2) Kwon, Y.-K., Kim, P. *Unusually High Thermal Conductivity in Carbon Nanotubes*; Springer: New York, 2006; p 227.
(3) Mamunya, Y. P.; Davydenko, V. V.; Pissis, P.; Lebedev, E. V. *Eur. Polym. J.* **2002**, *38*, 1887−1897.
(4) Yorifuji, D.; Ando, S. *Macromol. Chem. Phys.* **2010**, *211*, 2118−2124.
(5) Zhi, C.; Bando, Y.; Terao, T.; Tang, C.; Kuwahara, H.; Golberg, D. *Adv. Funct. Mater.* **2009**, *19*, 1857−1862.
(6) Song, W.-L.; Wang, P.; Cao, L.; Anderson, A.; Meziani, M. J.; Farr, A. J.; Sun, Y.-P. *Angew. Chem., Int. Ed.* **2012**, *51*, 6498−6501.
(7) Li, T.-L.; Hsu, S. L.-C. *J. Phys. Chem. B* **2010**, *114*, 6825−6829.
(8) Veca, L. M.; Meziani, M. J.; Wang, W.; Wang, X.; Lu, F.; Zhang, P.; Lin, Y.; Fee, R.; Connell, J. W.; Sun, Y.-P. *Adv. Mater.* **2009**, *21*, 2088−2092.
(9) Bozlar, M.; He, D.; Bai, J.; Chalopin, Y.; Mingo, N.; Volz, S. *Adv. Mater.* **2010**, *22*, 1654−1658.
(10) Song, S. H.; Park, K. H.; Kim, B. H.; Choi, Y. W.; Jun, G. H.; Lee, D. J.; Kong, B.-S.; Paik, K.-W.; Jeon, S. *Adv. Mater.* **2013**, *25*, 732−737.
(11) Balandin, A. A. *Nat. Mater.* **2011**, *10*, 569−581.
(12) Shahil, K. M. F.; Balandin, A. A. *Nano Lett.* **2012**, *12*, 861−867.
(13) Yaws, C. L. *Handbook of Thermal Conductivity: Inorganic Compounds and Elements*; Gulf Publishing Company: 1997; Vol. *4*, p 1.
(14) Mark, J. *Polymer data handbook*; Oxford University Press: New York, 2009; p 1.
(15) Yorifuji, D.; Ando, S. *J. Mater. Chem.* **2011**, *21*, 4402−4407.

(16) Zhou, T.; Wang, X.; Liu, X.; Xiong, D. *Carbon* **2010**, *48*, 1171−1176.
(17) Lee, E.-S.; Lee, S.-M.; Shanefield, D. J.; Cannon, W. R. *J. Am. Ceram. Soc.* **2008**, *91*, 1169−1174.
(18) Hill, R. F.; Supancic, P. H. *J. Am. Ceram. Soc.* **2002**, *85*, 851−857.
(19) Tanimoto, M.; Yamagata, T.; Miyata, K.; Ando, S. *ACS Appl. Mater. Interfaces* **2013**, *5*, 4374−4382.
(20) Tian, X.; Itkis, M. E.; Bekyarova, E. B.; Haddon, R. C. *Sci. Rep.* **2013**, *3*, 1710−1715.
(21) Haggenmueller, R.; Guthy, C.; Lukes, J. R.; Fischer, J. E.; Winey, K. I. *Macromolecules* **2007**, *40*, 2417−2421.
(22) Cho, H.-B.; Tokoi, Y.; Tanaka, S.; Suematsu, H.; Suzuki, T.; Jiang, W.; Niihara, K.; Nakayama, T. *Compos. Sci. Technol.* **2011**, *71*, 1046−1052.
(23) Sato, K.; Horibe, H.; Shirai, T.; Hotta, Y.; Nakano, H.; Nagai, H.; Mitsuishi, K.; Watari, K. *J. Mater. Chem.* **2010**, *20*, 2749−2752.
(24) Chen, Y.-M.; Ting, J.-M. *Carbon* **2002**, *40*, 359−362.
(25) Grove, S. M. *Compos. Sci. Technol.* **1990**, *38*, 199−209.
(26) Noor, A. K.; Shah, R. S. *Compos. Struct.* **1993**, *26*, 7−23.
(27) Progelhof, R. C.; Throne, J. L.; Ruetsch, R. R. *Polym. Eng. Sci.* **1976**, *16*, 615−625.
(28) Narkis, M.; Yacubowicz, J.; Vaxman, A.; Marmur, A. *Polym. Eng. Sci.* **1986**, *26*, 139−143.
(29) Reich, S. *J. Mater. Sci.* **1987**, *22*, 3391−3394.
(30) Huang, H.; Liu, C. H.; Wu, Y.; Fan, S. *Adv. Mater.* **2005**, *17*, 1652−1656.
(31) Marconnet, A. M.; Yamamoto, N.; Panzer, M. A.; Wardle, B. L.; Goodson, K. E. *ACS Nano* **2011**, *5*, 4818−4825.
(32) Gelves, G. A.; Lin, B.; Sundararaj, U.; Haber, J. A. *Adv. Funct. Mater.* **2006**, *16*, 2423−2430.